Integrative and Comparative Biology, volume 51, number 5, pp. 666–675
doi:10.1093/icb/icr111

SYMPOSIUM

The World Is not Flat: Defining Relevant Thermal Landscapes in the Context of Climate Change

Michael W. Sears,[1,*] Evan Raskin* and Michael J. Angilletta Jr[†]

*Department of Biology, Bryn Mawr College, 101 N. Merion Ave., Bryn Mawr, PA 19010, USA; [†]School of Life Sciences, Arizona State University, Tempe, AZ 85287, USA

From the symposium "A Synthetic Approach to the Response of Organisms to Climate Change: The Role of Thermal Adaptation" presented at the annual meeting of the Society for Integrative and Comparative Biology, January 3–7, 2011, at Salt Lake City, Utah.

[1]E-mail: msears@brynmawr.edu

Synopsis Although climates are rapidly changing on a global scale, these changes cannot easily be extrapolated to the local scales experienced by organisms. In fact, such generalizations might be quite problematic. For instance, models used to predict shifts in the ranges of species during climate change rarely incorporate data resolved to $<1\,km^2$, although most organisms integrate climatic drivers at much smaller scales. Empirical studies alone suggest that the operative temperatures of many organisms vary by as much as 10–20°C on a local scale, depending on vegetation, geology, and topography. Furthermore, this variation in abiotic factors ignores thermoregulatory behaviors that many animals use to balance heat loads. Through a set of simulations, we demonstrate how variability in elevational topography can attenuate the effects of warming climates. These simulations suggest that changing climates do not always impact organisms negatively. Importantly, these simulations involve well-known relationships in biophysical ecology that show how no two organisms experience the same climate in the same way. We suggest that, when coupled with thermoregulatory behavior, variation in topographic features can mask the acute effect of climate change in many cases.

Introduction

As climates change rapidly at both regional and global scales, biologists are faced with the challenge of predicting the responses of ecological systems (IPCC 2007; Pereira et al. 2010). One class of problems has focused on the responses of species to anticipated changes in temperature and precipitation (Elith and Leathwick 2009; Franklin 2009). Indeed, many models have been developed recently to predict both contemporary ranges of species and future shifts in range, largely based on the concept of the fundamental niche. These models can be broadly divided into statistical (e.g., Elith et al. 2006; Guisan et al. 2007b) and mechanistic approaches (e.g., Porter et al 2002; Buckley et al. 2010). Although practitioners of both approaches consider environmental variables at local scales when predicting the limits of species' ranges, the requirements of data and ease of implementation of the two approaches differ dramatically. Statistical models are attractive because they simply relate geo-referenced climate data (as well as other data available from Geographic Information Systems) to the presences and absences of a species, without the need to specify detailed biological mechanisms. On the other hand, mechanistic approaches are potentially more robust because they characterize niches from the principles of heat and mass balance. Using this approach, persistence of a species at any geographical location is modeled by explicitly linking local climates (past, present, or future) to the physiological and behavioral performances of individuals and (in some cases) to the dynamics of populations (Kearney and Porter 2004; Crozier and Dwyer 2006; Buckley 2008).

Recently, Buckley et al. (2010) compared the performances of several statistical and mechanistic models. From this comparison, two points emerged. First, although statistical models tended to predict

Advanced Access publication September 21, 2011

current ranges rather well, they did not predict dramatic shifts in ranges expected under typical scenarios of climate change. Second, although mechanistic models seemed sensitive to contemporary and future climates, predicted ranges depended on the types of mechanisms used to define the persistence of a population. The failure of statistical models to predict geographic ranges during climate change likely arose simply because models are confronted with novel climates for which there are no modern analogs (Williams and Jackson 2007; Suding et al. 2008). Unfortunately, there may be no solution to this problem, no matter how sophisticated the statistical approach. Because mechanistic approaches model fundamental niches independently of historical climates, their predictions are more or less immune to the problem presented by novel climates.

That said, mechanistic models suffer from a long list of issues that affect the accuracy of their predictions. With respect to biological realism, mechanistic models generally have ignored historical effects and species' interactions (Jackson et al. 2009; Gilman et al. 2010). Dispersal and migration, including the inability to overcome barriers (Massot et al. 2008; Carvalho 2010), are rarely considered. The acclimation or adaptation of physiology and behavior (as a dynamic process) are typically ignored as well (Chevin et al. 2010). But, even if these biological processes were considered, mechanistic models would still suffer from two problems with regard to their representation of the environment. First, the spatial scales of the environment in the models greatly exceed the scales actually experienced by organisms. The most readily and freely available data for climate modeling are resolved at scales from 30 m to 1 km (e.g., WORLDCLIM data); yet, many organisms experience environmental heterogeneity on scales of less than a meter (e.g., Helmuth 1998). Despite the mismatch between scales, models formulated for the same species at different spatial resolutions can predict inconsistent patterns (Guisan et al. 2007a; Trivedi et al. 2008). The second problem is that most organisms do not experience the climatic conditions recorded at weather stations, but rather as some integration of those conditions. Together, air temperature, radiation, surface temperature, and wind speed determine the operative temperature of an organism of a particular shape, size, and color (Bakken 1992; Dzialowski 2005). Therefore, operative temperature is a more appropriate index of the environmental conditions surrounding an organism than is air temperature. Additionally, landscape features will influence the drivers of operative temperature. Although some mechanistic models implicitly incorporate such factors (topography, vegetation, etc.) into their calculations (e.g., Porter et al. 2002), we believe that an explicit treatment of such factors might reveal the extent to which they contribute to the thermal heterogeneity of an environment. Given these two problems, mechanistic models have failed to accurately portray environments in terms of the magnitude of climatic variables and their heterogeneity through space and time, which are of importance to the thermoregulatory performance of individuals.

In this article, we examine how spatial heterogeneity can impact biological responses to thermal landscapes at scales that are more relevant to organisms. Specifically, we examine the effects of topographic relief on the range of operative temperatures available for behavioral thermoregulation and physiological performance. We show that, given identical climatic data, landscapes with increasing topographic relief produce thermal heterogeneity for small organisms that can be exploited for thermoregulation. Consequently, topographic relief provides increased potential for activity under contemporary climates, and such properties of landscapes might ameliorate some negative effects of climate change. Given that current models of species' ranges assume homogeneity of topography over scales that exceed those pertaining to organisms, we suggest that future iterations of such models consider the topographical properties of landscapes at much smaller resolutions.

Methods

To explore the effects of topography on operative temperatures, we constructed three artificial landscapes that differed in elevational relief. First, an artificial fractal landscape was constructed using the r.surf.fractal tool in GRASS GIS (GRASS Development Team 2010). This tool creates a simulated land surface of a specified fractal dimension (Saupe 1988). The generated fractal surface is represented as a set of raster data containing elevations for each pixel of the resulting map. Landscapes for this simulation were devoid of vegetation. Resulting landscapes were represented by a 100-pixel by 100-pixel grid, where the spatial resolution of each pixel in the grid was 1.0×1.0 m. We chose this spatial scale to illustrate the effects of topography, but an even finer resolution is likely to be more appropriate for the scale of environmental heterogeneity experienced by many organisms. To create different topographies, we either compressed or expanded the elevational range of the original surface by scaling each pixel

to fit a specified range. Here, we created a flat landscape with an elevational range of 1 m, a bumpy landscape with an elevational range of 4 m, and a hilly landscape with an elevational range of 16 m. Once these topographies were created, we generated corresponding raster maps of slopes and aspects using the r.slope.aspect tool in GRASS GIS (Hofierka et al. 2009). These three layers of data were used as the topographic inputs in a simple biophysical model (see Appendix) that predicts the operative temperatures of a small lizard (e.g., *Sceloporus undulatus*).

To predict operative temperatures over the different artificial landscapes, we coupled the topographic data with a series of climate data for a day in June at an arbitrarily chosen site in New Mexico, USA (coordinates: 34°N, 106°W). Operative temperatures were calculated as a function of microclimatic and organismal properties (Bakken 1992; Campbell and Norman 1998). Daily profiles of air temperatures were modeled from daily maximal and minimal temperatures (Campbell and Norman 1998). For simplicity, ground temperatures were assumed to be similar to air temperatures and wind speeds were set to 0.1 m/s for all simulations. We acknowledge that topography might also influence prevailing wind patterns; however, wind speeds are lower at the ground surface, which lessens the impact of wind speed (versus that of radiation) on operative temperature. Thus, the thermal heterogeneity modeled here represents a conservative estimate, but makes the point that surface topography matters.

Radiation incident to a flat plane was modeled using standard equations, which consider geographic location, time of day, and day of year (see Gates 1980). To model changes in incident radiation on surfaces that varied in slope and aspect, we calculated an angle of incidence, which was then substituted for the zenith angle (if the sun was above the horizon) to adjust radiation through the cosine law (Gates 1980). To further attenuate radiation at the surface, we modeled shadows cast by hills at every pixel and at each time step (Dozier et al. 1981; Dubayah and Rich 1995). If a pixel was shaded, the shortwave terms in the function of operative temperature were set to zero. For this set of simulations, we modeled an operative temperature for each pixel (1-m^2) once every 15 min. Additional information about this model can be found in the Appendix.

Once operative temperatures were calculated, we used the resultant maps to infer potential activity and energetics for each topography. For a cursory analysis of activity, temperatures were classified into two categories: those that fell within the range of temperatures suitable for surface activity and those that exceeded the critical thermal maximum for a "typical" lizard. We assumed that a range of 29–37°C permits activity, which roughly corresponds to the range of temperatures for active lizards (*Sceloporus* spp.) in temperate regions of North America (Crowley 1985; Angilletta 2001; Sears 2005). We used a critical thermal maximum of 41°C (Angilletta et al. 2002). Lizards were considered active if any pixel had an operative temperature within the bounds set for surface activity. Similar assumptions characterize most eco-physiological models of activity (e.g., Kearney and Porter 2004; Buckley 2008). Lastly, we created a map of potential energy gain by transforming temperatures through a simple bioenergetic model (Grant and Porter 1992). To examine the effect of a changing climate on thermal landscapes (and its consequences), we simulated operative temperatures for contemporary climates (based on historical weather data), as well as for a warming scenario (+3°C above historical conditions). All simulations were programmed using the Python programming language along with the NumPy library (Oliphant 2007).

Results and discussion

We hoped to make three major points by considering the effects of elevational topography on thermal heterogeneity in spatially explicit, realistic landscapes. First, identical climates can produce very different microclimates at the spatial scales experienced by organisms. Second, greater topographic relief should decrease selective pressure on thermal physiology for organisms that use behavior to avoid thermal extremes in heterogeneous environments (Huey et al. 2003). Third, topographic diversity should buffer the impacts of climate change by facilitating behavioral thermoregulation.

Thermal heterogeneity at small scales increases with topographic relief of the local environment, even under identical local climates (Fig. 1). One can easily detect this pattern among three simulated landscapes for a typical summer morning (Fig. 2). For a flat environment, operative temperatures do not vary appreciably throughout space at any point in time (Fig. 1). The mean range of temperatures at any instance throughout the day is 1.37 ± 1.18°C (mean ± standard deviation). Thus, both behavioral thermoregulation and physiological performance will be highly constrained in flat environments (all else being equal). For habitats with greater topographic relief, the range of operative temperatures throughout space increases at any given time. Mean ranges of

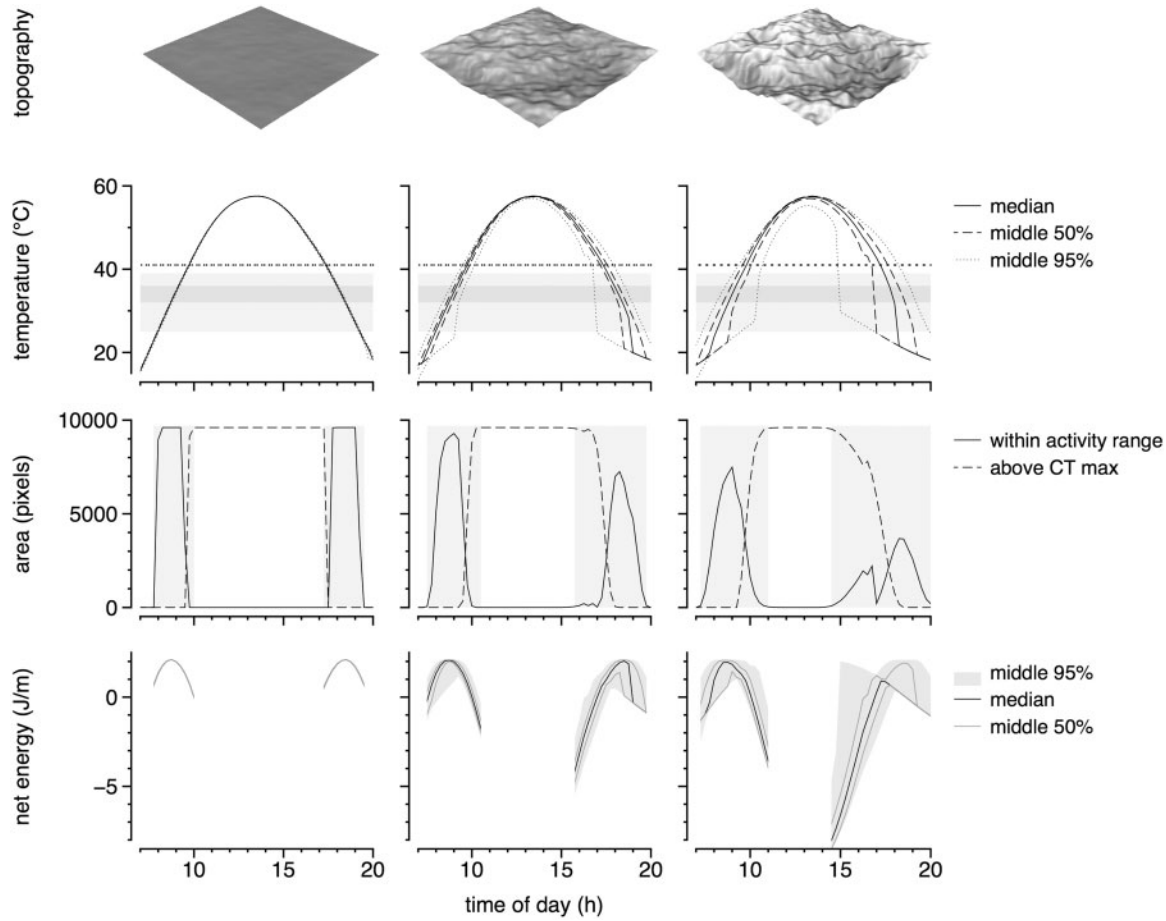

Fig. 1 (**A**) Flat, bumpy, and hilly topographies were created to examine the effects of elevational relief on thermal landscapes. (**B**) For each topography, operative temperatures were modeled at 15-min intervals for the 170th day of the year. In each plot, the median temperature as well as the middle 50% and middle 95% of temperatures are plotted across the day. The dark gray area represents temperatures within a lizard's preferred range of temperatures (32–36°C), and the light gray area represents the temperatures suitable for surface activity (29–37°C). (**C**) From these operative temperatures, we plotted the areas that fell within the range required for surface activity as well as the areas of habitat that exceeded the critical thermal maximum. Shaded areas represent the times of day when surface activity was possible. As elevational relief increases, potential activity increases and the interval between peaks in activity decreases. (**D**) As a consequence of operative temperatures, potential gains in energy (assuming a full gut) are plotted. Increased elevational relief confers the potential for increased energetic gains.

temperatures are 12.20 ± 8.51°C in the bumpy habitat and 17.37 ± 6.91°C in the hilly habitat.

Thermal heterogeneity might enable organisms to extend their activity by selecting preferred microclimates, resulting in longer exposure to temperatures that maximize physiological performance. That said, preferred microclimates become more patchily distributed as topographic relief increases (Fig. 2). In flat areas, preferred microclimates are either present or absent at virtually all sites within the landscape, depending on the time of day. Thus, while the task of locating preferred microclimates will be trivial at certain times of the day, these windows of time are limited. With increasing topographic relief, the potential duration of activity increases (flat: 4.5 h; bumpy: 7.00 h; hilly: 9.25 h), but a smaller portion of the landscape contains preferred microclimates during windows of time that permit activity. Generally, individuals can be active at earlier and later periods of the day because particular slopes and aspects favor higher incident radiation than do flat surfaces. Likewise, activity can extend into warmer parts of the day in bumpier habitats, because of the presence of shadows and angles of incidence that reduce incident radiation relative to that of a flat surface. Furthermore, thermal heterogeneity can decrease the duration between morning and evening peaks in activity, particularly during midsummer. Thus, topographic relief extends the potential time for activity beyond that in a flat landscape, with the tradeoff that not all parts of the landscape will be suitable during activity.

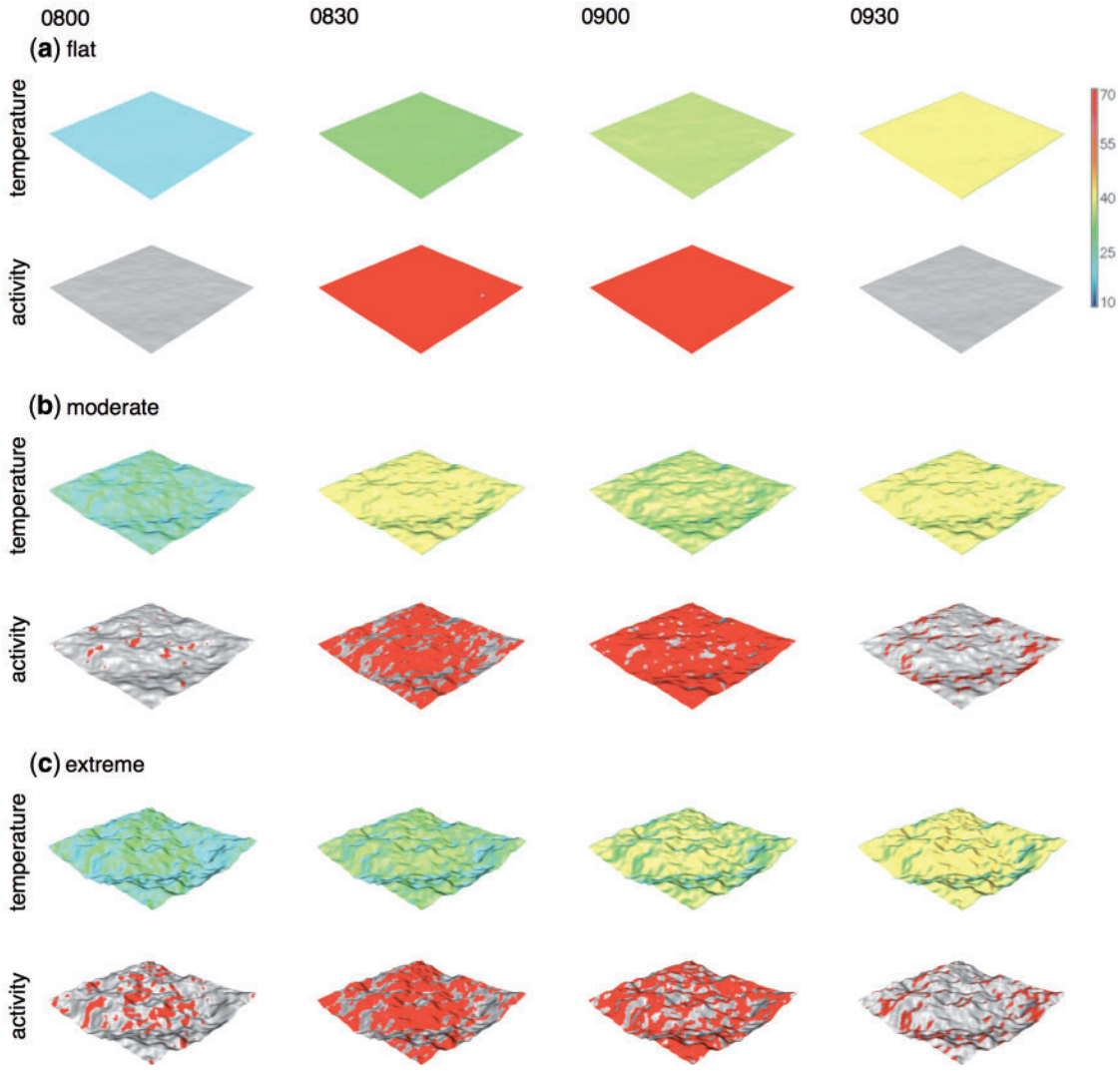

Fig. 2 Maps of operative temperatures and areas for potential surface activity for the flat, bumpy, and hilly topographies. For the flat topography (**a**), there is little thermal heterogeneity. As a consequence, there is only a narrow window for activity. However, when activity is possible, all areas within the landscape are suitable. Similar maps are shown for bumpy (**b**) and hilly (**c**) topographies. As the elevational relief increases, thermal heterogeneity increases. As a result, periods of potential activity become more spread out over time, and areas for surface activity become more limited over space.

Why does thermal heterogeneity matter? In addition to extending opportunities for activity, thermal heterogeneity also determines the cost of behavioral thermoregulation (Huey and Slatkin 1976; reviewed by Angilletta 2009). In a related set of simulations, which focused on a lizard's ability to thermoregulate in various landscapes, we found that the spatial distribution of temperatures affects the energetic cost of thermoregulation even when the statistical distribution of temperatures remains constant (see Chapter 4 of Angilletta 2009). When preferred microclimates were more distributed throughout an area, and hence distances between them were smaller, individuals could thermoregulate more effectively while expending less energy on movement. Consequently, thermoregulatory benefits were lower and energetic costs were higher in environments where preferred microclimates were harder to locate. Although we still do not know whether these results translate to natural environments, we believe that understanding the costs of thermoregulation will help us to predict the activity of organisms.

All else being equal, how might changes in thermal heterogeneity created by environmental warming influence the activity and energetics of organisms?

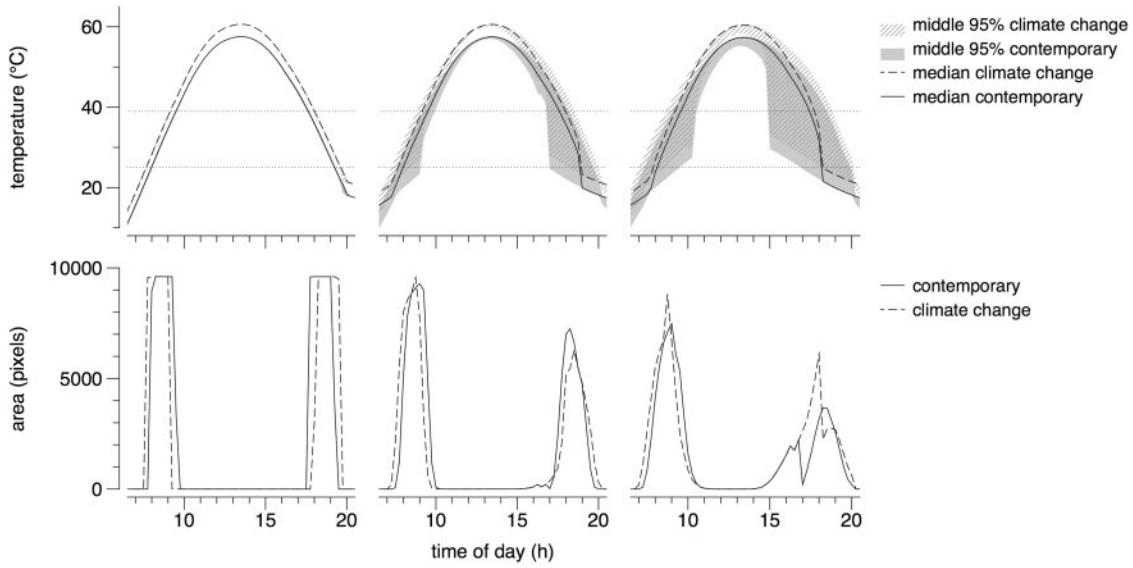

Fig. 3 The potential effects of increasing environmental temperatures on thermal landscapes depends on the topographic structure of the environment. (**A**) Median operative temperatures and the middle 95% of operative temperatures are plotted for each surface. The shaded areas with cross-hatching represents the middle 95% of operative temperatures under contemporary conditions while the unshaded areas with cross-hatching represent the same conditions under a scenario of climate change. The horizontal dotted line represents the critical thermal maximum for a lizard. (**B**) Potential areas for surface activity are plotted under contemporary scenarios as well as scenarios of climate change. For the flat topography, time and space for activity are relatively unchanged, but the interval between peaks in activity increases after climate change. For the bumpy habitat, changes in total activity are minimal as are shifts in activity periods. In the hilly habit, lizards gain potential area for surface activity although the times available for activity remain relatively unchanged.

Warming will likely matter in two ways. On a proximate level, warming could influence how patterns of activity shift during climate change. On an ultimate level, warming could influence selective pressures that shape behavior and physiology in future climates. In our model, the potential duration of activity did not differ much between contemporary climatic conditions and a scenario of climate change, in which 3°C was added to air temperature (Fig. 3). What did differ was the duration between potential bouts of activity. Preferred microclimates appeared earlier in the morning and disappeared later in the evening. Since individuals in nature would likely remain warm during periods of midday inactivity, climate change should increase energy expenditure over the course of a day without increasing opportunities to forage. Depending on the magnitude of this effect (and the behavioral responses of prey), climate change could decrease the energy available for growth and reproduction. Interestingly, the impact of climate change on potential activity should be ameliorated by topographic relief, because of the way that relief extends the potential period of activity during midday. Interestingly, in the hilly topography, space for surface activity increased under climate change without much change in the potential timing of activity. Possibly, individuals in hilly landscapes would benefit from environmental warming. This result stresses the importance of considering microclimatic variation when attempting to understand responses to climate change.

Thermal heterogeneity also will affect the selective pressures on the thermal sensitivities of organismal phenotypes, and understanding these selective pressures will be critical for predicting responses to changing climates. Indeed, models that attempt to predict the evolution of thermal sensitivity are in their infancy and, to date, generally have not allowed for thermoregulation (reviewed by Angilletta et al. 2002; Angilletta 2009). Relaxing this assumption will be a nontrivial endeavor given that many factors determine an organism's motivation and ability to thermoregulate. That said, we can ponder the potential interactive effects of environmental warming and topographical relief on the evolution of thermal sensitivities. Current models, which assume no thermoregulation, predict that stable environments (e.g., tropical regions) select for thermal specialists with little margin of safety between their optimal temperature for performance and the maximal temperature they can tolerate (Lynch and Gabriel 1987; Gilchrist 1995; Deutsch et al. 2008). For organisms in flatter environments, where thermoregulation cannot occur,

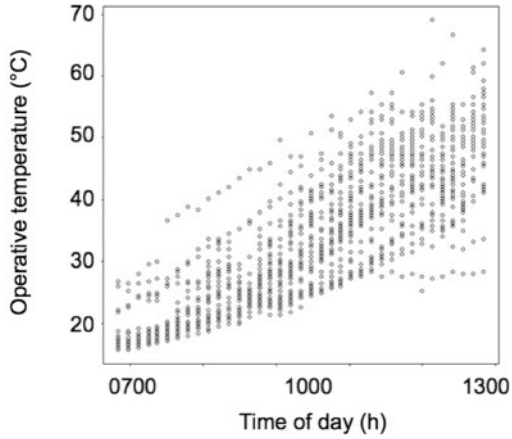

Fig. 4 Operative temperature recorded by hollow, copper replicas of a small lizard (based on an adult *Sceloporus undulatus*) are shown for a typical June day in an area with moderate topographic relief in the Mescalero sand dunes in New Mexico. Operative temperatures can range over 20°C depending on slope, aspect, and vegetation.

responses to changing climates might be expected to parallel those of thermoconformers. For organisms in hilly environments, which experience more spatial heterogeneity of microclimates, we might expect behavioral thermoregulation to buffer changes in the mean or maximal temperature. Behavioral thermoregulation can weaken selection on thermal sensitivity (Huey et al. 2003), particularly if expected increases in mean air temperature are small, relative to the spatial variation in operative temperature (Clusella-Trullas and Chown 2011). For example, operative temperature can vary by tens of degrees at a given instance in time in a complex environment (Fig. 4). Such spatial heterogeneity enables *Sceloporus* lizards to maintain very similar body temperatures during activity over broad geographic ranges (Andrews 1998). Thermoregulating species, by minimizing their exposure to thermal variation, reduce their potential to adapt to climate change. Thus, the buffering of thermal heterogeneity through behavior ultimately puts a species at risk once it exhausts behavioral options for coping with environmental warming.

The simple mapping of operative temperatures onto landscapes, as illustrated here, is only the first step toward understanding how organisms respond to warming environments. Such maps of thermal landscapes should be viewed as inputs to models that link the magnitude and thermal heterogeneity to the persistence of populations. These models should account not just for behavioral and physiological responses to temperature, but also for the impacts of spatial distributions of temperatures. Researchers have made significant progress along this front and, in many respects, have been limited by the scale of spatial data available for modeling (Kearney and Porter 2004; Buckley 2008). Even so, the spatially explicit processes that influence the persistence of populations are lacking in these models. For instance, organisms do not move among microhabitats (i.e., pixels) to thermoregulate or to meet energetic demands. Furthermore, interactions with nonthermal resources, such as those related to hydration and nutrition, should be considered as well. Although ecologists understand many of the processes that limit species' ranges (Sexton et al. 2009), and have made significant progress in developing tools to aid in their prediction (Franklin 2009), theorists and empiricists need to work together if future iterations of these models are to improve significantly. Empiricists need to record data not only in a spatial context, but also with regard to how biological processes influence organisms' use of space. For instance, how does the ability to forage or disperse trade off with the need to thermoregulate? Furthermore, theoreticians need to construct models that not only use the data collected by empiricists but also suggest what additional data should be collected. A coordinated effort amongst scientists with complementary skills will be necessary to explain and predict the biological impacts of changing landscapes (Angilletta and Sears 2011).

Acknowledgments

We thank the physiological ecologists who pioneered the conceptual advances that led to our work, including Raymond Huey, Art Dunham, George Bakken, Richard Tracy, and Warren Porter. We also thank members of the Species Range Dynamics working group (supported by the National Center for Ecological Analysis and Synthesis and the National Evolutionary Synthesis Center) for conversations that helped to focus some of the points made in this article.

Funding

The National Science Foundation (DBI-0204484, IOS-0616176, IOS 0616344, CCF-0939370).

References

Andrews RM. 1998. Geographic variation in field body temperature of *Sceloporus* lizards. J Therm Biol 23:329–34.

Angilletta MJ. 2001. Thermal and physiological constraints on energy assimilation in a widespread lizard (*Sceloporus undulatus*). Ecology 82:3044–56.

Angilletta MJ. 2009. Thermal adaptation: a theoretical and empirical synthesis. Oxford: Oxford University Press.

Angilletta MJ, Hill T, Robson MA. 2002. Is physiological performance optimized by thermoregulatory behavior? A case study of the eastern fence lizard, *Sceloporus undulatus*. J Therm Biol 27:203–8.

Angilletta MJ, Sears MW. 2011. Coordinating theoretical and empirical efforts to understand the linkages between organisms and environments. Integr Comp Biol 51: 653–61.

Bakken GS. 1992. Measurement and application of operative and standard operative temperatures in ecology. Am Zool 32:194–216.

Buckley LB. 2008. Linking traits to energetics and population dynamicsto predict lizard ranges in changing environments. Am Nat 171:E1–19.

Buckley LB, Urban MC, Angilletta MJ, Crozier LG, Rissler LJ, Sears MW. 2010. Can mechanism inform species' distribution models? Ecol Lett 13:1041–54.

Campbell GC, Norman JN. 1998. Introduction to environmental biophysics. 2nd ed. Berlin: Springer.

Carvalho SB, Brito JC, Crespo EJ, Possingham HP. 2010. From climate change predictions to actions–conserving vulnerable animal groups in hotspots at a regional scale. Glob Change Biol 16:3257–70.

Chevin LM, Lande R, Mace GM. 2010. Adaptation, plasticity, and extinction in a changing environment: towards a predictive theory. PLoS Biol 8:e1000357.

Clusella-Trullas S, Chown SL. 2011. Comment on ''Erosion of Lizard Diversity by climate change and altered thermal niches.'' Science 332:537.

Crowley SR. 1985. Thermal sensitivity of sprint-running in the lizard *Sceloporus undulatus*: support for a conservative view of thermal physiology. Oecologia 66:219–25.

Crozier L, Dwyer G. 2006. Combining population dynamic and ecophysiological models to predict climate-induced insect range shifts. Am Nat 167:853–66.

Deutsch CA, Tewksbury JJ, Huey RB, Sheldon KS, Ghalambor CK, Haak DC, Martin PR. 2008. Impacts of climate warming on terrestrial ectotherms across latitude. Proc Natl Acad Sci 105:6669–72.

Dozier J, Bruno J, Downey P. 1981. A faster solution to the horizon problem. Comput Geosci 7:145–51.

Dubayah R, Rich PM. 1995. Topographic solar radiation models for GIS. Int J Geogr Inf Sci 9:405–19.

Dzialowski EM. 2005. Use of operative temperature and standard operative temperature models in thermal biology. J Therm Biol 30:317–34.

Elith J, Leathwick JR. 2009. Species distribution models: ecological explanation and prediction across space and time. Annu Rev Ecol Syst 40:677–97.

Elith J, et al. 2006. Novel methods improve prediction of species' distributions from occurrence data. Ecography 29:129–51.

Franklin J. 2009. Mapping species distributions: spatial inference and prediction. Cambridge: Cambridge University Press.

Gates DG. 1980. Biophysical ecology. New York: Springer.

Gilchrist GW. 1995. Specialists and generalists in changing environments I: fitness landscapes of thermal sensitivity. Am Nat 146:252–70.

Gilman SE, Urban MC, Tewksbury J, Gilchrist GW, Holt RD. 2010. A framework for community interactions under climate change. Trends Ecol Evol 25:325–31.

Grant BW, Porter WP. 1992. Modeling global macroclimatic constraints on ectotherm energy budgets. Am Zool 32:154–78.

GRASS Development Team. 2010. *Geographic Resources Analysis Support System (GRASS) Programmer's Manual*. Open Source Geospatial Foundation. http://grass.osgeo.org/programming6/.

Guisan A, Graham CH, Elith J, Huettmann F. 2007a. Sensitivity of predictive species distribution models to change in grain size. Diversity Distributions 13:332–40.

Guisan A, Zimmerman NE, Elith J, Graham CH, Phillips S, Peterson AT. 2007b. What matters for predicting the occurrences of trees: techniques, data, or species characteristics. Ecol Monogr 77:615–30.

Helmuth BST. 1998. Intertidal mussel microclimates: predicting the body temperature of a sessile invertebrate. Ecol Monogr 68:51–74.

Hofierka J, Mitaso H, Neteler M. 2009. Geomorphometry in GRASS GIS. In: Hengl T, Reuter HI, editors. Geomorphometry: concepts, software, applications. Developments in soil science, Vol. 33. Amsterdam: Elsevier. p. 387–410.

Huey RB, Hertz PE, Sinervo B. 2003. Behavioral drive versus behavioral inertia in evolution: a null model approach. Am Nat 161:357–66.

Huey RB, Slatkin M. 1976. Costs and benefits of lizard thermoregulation. Q Rev Biol 51:363–84.

IPCC. 2007. Climate Change 2007: The physical science basis. In: Solomon S, Qin D, Manning M, Chen Z, Marquis Z, Averyt KB, Tignor M and Miller HL, editors. Contribution of Working Group I to the Fourth Assessment Report of the Intergovernmental Panel on Climate Change. Cambridge; New York, NY: Cambridge University Press.

Jackson ST, Betancour JL, Booth RK, Gray ST. 2009. Ecology and the ratchet of events: climate variability, niche dimensions, and species distributions. Proc Natl Acad Sci USA 106(Suppl. 2):19685–92.

Kearney M, Porter WP. 2004. Mapping the fundamental niche: physiology, climate, and the distribution of a nocturnal lizard. Ecology 85:3119–31.

Lynch M, Gabriel W. 1987. Environmental tolerance. Am Nat 129:283–303.

Massot M, Clobert J, Ferriere REG. 2008. Climate warming, dispersal inhibition and extinction risk. Glob Change Biol 14:461–9.

McCullough EC, Porter WP. 1971. Computing clear day solar radiation spectra for the terrestrial ecological environment. Ecology 52:1008–15.

Mitchell JW. 1976. Heat transfer from spheres and other animal forms. Biophys J 15:561–9.

Oliphant TE. 2007. Python for scientific computing. Comput Sci Eng 9:10–20.

Pereira HM, et al. 2010. Scenarios for global biodiversity in the 21st century. Science 330:1496–501.

Porter WP, Sabo JL, Tracy CR, Reichman OJ, Ramankutty N. 2002. Physiology on a landscape scale: plant-animal interactions. Integr Comp Biol 42:431–53.

Saupe D. 1988. Algorithms for random fractals. In: Barnsley M, Devaney R, Mandelbrot B, Peitgen H-O, Saupe D, Voss R, editors. The science of fractal images, Ch. 2. London: Springer. p. 71–136.

Sears MW. 2005. Geographic variation in the life history of the sagebrush lizard: the role of thermal constraints on activity. Oecologia 143:25–36.
Sexton JP, McIntyre PJ, Angert AL, Rice KJ. 2009. Evolution and ecology of species range limits. Annu Rev Ecol Evol Syst 40:415–36.
Suding KN, Lavorel S, Chapin FS, Cornelissen JHC, Diaz S, Garnier E, Goldberg D, Hooper DU, Jackson ST, Navas ML. 2008. Scaling environmental change through the community-level: a trait-based response-and-effect framework for plants. Glob Change Biol 14:1125–40.
Trivedi MR, Berry PM, Morecroft MD, Dawson TP. 2008. Spatial scale affects bioclimate model projections of climate change impacts on mountain plants. Glob Change Biol 14:1089–1103.
Williams JW, Jackson ST. 2007. Novel climates, no-analog communities, and ecological surprises. Front Ecol Environ 5:475–82.

Appendix

Appendix 1 Operative temperature model

To create thermal landscapes, we calculated operative environmental temperatures for each pixel in our simulated landscape. Operative environmental temperatures (T_e) for a flat surface were calculated as

$$T_e = T_a + \frac{R_{abs} - \varepsilon_s \sigma (T_a + 273.15)^4}{c_p (g_r + g_{Ha})} \quad (1)$$

where T_a is the air temperature, ε_s is the emissivity of the animal, σ is the Stephan–Bolzmann constant, c_p is the specific heat of air at constant pressure, g_r is the radiative conductance of the animal, and g_{Ha} is the boundary layer conductance for heat (Bakken 1992; Campbell and Norman 1998). R_{abs} is fairly detailed and is presented below. g_r is calculated as

$$g_r = \frac{4\sigma (T_a + 273.15)^3}{c_p} \quad (2)$$ (Campbell and Norman 1998)

g_{Ha} is calculated as

$$g_{Ha} = 1.4 \cdot 0.135 \sqrt{\frac{u}{d}} \quad (3)$$

where u is the wind speed and d is the characteristic dimension of the animal (Campbell and Norman 1998; Mitchell 1976).

Radiation submodel

Radiation absorbed (R_{abs}) by an animal was calculated as

$$R_{abs} = s \cdot \alpha_s (F {}_hS_0 + 0.5 S_d + 0.5 S_r) + 0.5 \alpha_l (S_{l,a} + S_{l,g}) \quad (4)$$

where s is the proportion of the animal in direct sun, α_s and α_l are the absorptivities of short- and long-wave radiation, F is the view factor of the organism, ${}_hS_0$ is the direct solar radiation reaching the earth surface, S_d is the diffuse radiation at the earth surface, S_r is the reflected radiation reflected form the earth surface, S_{la} is the longwave radiation emitted from the atmosphere, and $S_{l,g}$ is the longwave radiation emitted from the ground surface. (Gates 1980; Campbell and Norman 1998).

To determine the proportion of direct solar radiation reaching the animal, a view factor (F) was calculated as the ratio of shadow area on a surface that is perpendicular to the solar beam (A_p) to the total surface area of a cylinder with rounded ends (A) as

$$F = \frac{A_p}{A} = 1 + \frac{\frac{4h \sin\theta}{\pi d}}{4 + \frac{4h}{d}} \quad (5)$$

where h is the length of the cylinder, d is the diameter of the cylinder, and θ is the angle between the solar beam and the longitudinal axis of the animal (Campbell and Norman 1998).

The amount of direct solar radiation (${}_hS_0$) reaching the earth's surface was calculated as

$${}_hS_0 = \bar{S}_0 \left(\frac{\bar{d}}{d}\right)^2 \cos z \cdot \tau^m \quad (6)$$

where $\bar{S}_0$ is the solar constant ($1360\,\mathrm{W m^{-2}}$) (Gates 1980; Campbell and Norman 1998). τ^m corrects for transmittance through the atmosphere, where τ is the optical transmittance and m is the optical air mass number. m is calculated as

$$m = \frac{p_a}{101.3 \cos z} \quad (7)$$

where p_a is the air pressure and z is the zenith angle (Campbell and Norman 1998). p_a is estimated as

$$P_a = 101.3 e^{\frac{a}{8200}} \quad (8)$$

where a is the altitude in meters (Campbell and Norman 1998). $\left(\frac{\bar{d}}{d}\right)^2$ is a correction factor that accounts for the elliptical orbit of the earth. This factor is calculated as

$$\left(\frac{\bar{d}}{d}\right)^2 = 1 + 2 \cdot 0.1675 \cos\left(\frac{2\pi}{365} J\right) \quad (9)$$

where J is the Julian day of the year (McCullough and Porter 1971). Using the cosine law, $\cos z$ attenuates solar radiation across times of day given changes in the zenith angle (z), where z (in degrees)

is calculated as

$$z = \cos^{-1}(\sin\phi \sin\delta + \cos\phi \cos\delta \cos h) \quad (10)$$

where δ is the latitude, δ is the declination of the sun, and h is the hour angle of the sun (Gates 1980). Declination (ϕ) is calculated (in radians) as

$$\delta = \sin^{-1}(0.39785 \sin[278.97 + 0.9856 * J \sin(356.6 + 0.9856J)]) \quad (11)$$

where J is the Julian day (Campbell and Norman 1998). The hour angle (h, in degrees) is calculated as

$$h = 15(t - t_0) \quad (12)$$

where t is the time of the day and t_0 is solar noon. Solar noon is calculated as

$$t_0 = 12 - LC - ET \quad (13)$$

LC is the longitudinal correction, calculated as

$$LC = l \bmod 15 \quad (14)$$

where l is the longitude (Campbell and Norman 1998). ET is the equation of time calculated as

$$ET = \frac{\begin{array}{l} -104.7 \sin f + 596.2 \sin 2f + 4.3 \sin 3f \\ -12.7 \sin 4f - 429.3 \cos f \\ -2.0 \cos 2f + 19.3 \cos 3f \end{array}}{3600} \quad (15)$$

where f is calculated as

$$f = 279.575 + 0.9856J \quad (16) \text{ (Campbell and Norman 1998)}$$

The amount of diffuse radiation (S_d) is calculated as

$$S_d = {}_h\, S_0 \cdot 0.3(1 - \tau^m) \quad (17) \text{ (Campbell and Norman 1998; Gates 1980)}$$

The amount of reflected radiation (S_r) was calculated as

$$S_r = r_g h S_0 \quad (18)$$

where r_g is the ground albedo (Gates 1980; Campbell and Norman 1998).

Longwave radiation from the atmosphere ($S_{l,a}$) was calculated as

$$S_{l,a} = 53.1 \times 10^{-14}(T_a + 273.15)^6 \quad (19) \text{ (Campbell and Norman 1998)}$$

Longwave radiation ($S_{l,g}$) emitted from the ground was calculated as

$$S_{l,g} = \varepsilon_g \sigma (T_a + 273.15)^4 \quad (20) \text{ (Campbell and Norman 1998)}$$

To account for topographic relief at the earth's surface, we used the angle of incidence (i) in place of the zenith angle z in the above calculations. Note, we first calculated the zenith angle to ensure that the sun was above the horizon. The angle of incidence was calculated as

$$i = \cos^{-1}(\cos a_s \cos a \cos(\alpha - \alpha_s) + \sin a_s \sin a) \quad (21)$$

for $i \leq \frac{\pi}{2}$ radians (Gates 1980).

Otherwise, i was set to $\frac{\pi}{2}$ radians. Here, a is the altitude angle, α is the azimuth angle, a_s is the slope, and α_s is the aspect. The altitude angle was calculated as

$$a = \sin^{-1}(\sin\phi \sin\delta + \cos\phi \cos\delta \cos h) \quad (22)$$

and the azimuth angle was calculated as

$$\alpha = 180 - \cos^{-1}\left(\frac{-\sin\delta - \cos z \sin\phi}{\cos\phi \sin z}\right) \text{ for } t < t_0$$
$$\alpha = 180 - \cos^{-1}\left(\frac{-\sin\delta - \cos z \sin\phi}{\cos\phi \sin z}\right) \text{ for } t \geq t_0 \quad (23) \text{ (Gates 1980)}$$

For all calculations of operative temperature, because of elevational topography, we calculated whether or not a pixel fell in a shadow. This procedure was performed by determining (on a pixel by pixel basis) whether or not the solar vector (described in direction by the azimuth angle and in height above the ground by the altitude angle) was broken by a topographical feature. If so, then s in Equation (4) was set to zero (Dozier et al. 1981), effectively eliminating the shortwave radiation term from R_{abs}.

Air temperature submodel

Air temperatures were estimated from the following equations, which take daily minimum (T_n) and maximum air temperatures (T_x) as input. First, the dimensionless diurnal temperature function was calculated as

$$\Gamma(t) = 0.44 - 0.46 \sin(\omega t + 0.9) + 0.11 \sin(2\omega t + 0.9) \quad (24)$$

where t is the time of day and PM (Campbell and Norman 1998). Next, temperature for any time of day was calculated as

$$\begin{aligned} T(t) &= T_{x,i-1}\Gamma(t) + T_{n,i}[1 - \Gamma(t)] \quad \text{for } 0 < t \leq 5 \\ T(t) &= T_{x,i}\Gamma(t) + T_{n,i}[1 - \Gamma(t)] \quad \text{for } 5 < t \leq 14 \\ T(t) &= T_{x,i}\Gamma(t) + T_{n,i}[1 - \Gamma(t)] \quad \text{for } 14 < t < 24 \end{aligned} \quad (25)$$

using T_x and T_n relative to day i (using T_x for i and i-1 and T_n for i and i+1).